Quantum tautomerization in porphycene and its isotopomers: Path-integral molecular dynamics simulations

ARTICLE *in* CHEMICAL PHYSICS · FEBRUARY 2012

Impact Factor: 1.65 · DOI: 10.1016/j.chemphys.2011.12.007

5 AUTHORS, INCLUDING:

Yoshikawa Takehiro
Saitama University
14 PUBLICATIONS **101** CITATIONS
SEE PROFILE

Motoyuki Shiga
Japan Atomic Energy Agency
87 PUBLICATIONS **1,436** CITATIONS
SEE PROFILE

Chemical Physics 394 (2012) 46–51

Contents lists available at SciVerse ScienceDirect

Chemical Physics

journal homepage: www.elsevier.com/locate/chemphys

Quantum tautomerization in porphycene and its isotopomers: Path-integral molecular dynamics simulations

Takehiro Yoshikawa [a], Shuichi Sugawara [a], Toshiyuki Takayanagi [a,*], Motoyuki Shiga [b], Masanori Tachikawa [c]

[a] Department of Chemistry, Saitama University, Shimo-Okubo 255, Sakura-ku, Saitama City, Saitama 338-8570, Japan
[b] Center for Computational Science and E-systems, Japan Atomic Energy Agency, The University of Tokyo, 5-1-5, Kashiwanoha, Kashiwa City, Chiba 277-8563, Japan
[c] Quantum Chemistry Division, Graduate School of Nanobioscience, Yokohama-City University, Seto 22-2, Kanazawa-ku, Yokohama 236-0027, Japan

ARTICLE INFO

Article history:
Received 12 November 2011
In final form 14 December 2011
Available online 23 December 2011

Keywords:
Path-integral molecular dynamics simulation
Semiempirical electronic structure method
Proton transfer
Hydrogen-bond
Nuclear quantum effect
Porphycene

ABSTRACT

Path-integral molecular dynamics simulations have been performed for porphycene and its isotopic variants in order to understand the effect of isotopic substitution of inner protons on the double proton transfer mechanism. We have used an on-the-fly direct dynamics technique at the semiempirical PM6 level combined with specific reaction parameterization. Our quantum simulations show that double proton transfer of the unsubstituted porphycene at $T = 300$ K mainly occurs via a so-called concerted mechanism through the D_{2h} second-order saddle point. In addition, we found that both isotopic substitution and temperature significantly affect the double proton transfer mechanism. For example, the contribution of the stepwise mechanism increases with a temperature increase. We have also carried out hypothetical simulations with the porphycene configurations being completely planar. It has been found that out-of-plane vibrational motions significantly decrease the contribution of the concerted proton transfer mechanism.

1. Introduction

Multiple proton/hydrogen transfer is one of the fundamental chemical reactions and has been observed in a wide range of molecular systems [1,2]. A basic question to be solved is whether the transfer occurs via a concerted or stepwise pathway. In the concerted mechanism, multiple protons (or hydrogen atoms) simultaneously move, while in the stepwise mechanism single proton transfers consecutively occur with each transfer process being an independent event. There have been many discussions of the mechanism of double proton transfer processes in the past. For example, the question has been frequently addressed by using static electronic structure calculations of the potential energy surface of the system. When the barrier height for the concerted mechanism is lower than that of the stepwise mechanism, it can be qualitatively concluded that the former mechanism is preferred. However, this simplified picture cannot be applied without considering the dynamics of nuclei. Moreover, it should be mentioned that the potential energy surface of the double proton transfer reaction often contains second-order saddle points. In this case, it is sometimes difficult to locate such stationary points using standard quantum chemistry calculations.

In this work we focus on porphycene, a model system for studying intramolecular double proton transfer [3–9]. Porphycene, a constitutional isomer of porphyrin, has four pyrrole rings that form four protonable sites inside the cavity. Due to short distances between the inner nitrogen atoms and strong hydrogen-bonds, porphycene shows different tautomeric properties from porphyrin. In the case of porphyrin, it is known that the barrier height for the stepwise pathway is much lower than that for the concerted pathway [2,10]. Therefore, the dominant proton transfer pathway for porphyrin is considered to be the stepwise one. On the other hand, in the case of porphycene, the energy difference between the barrier heights of the concerted and stepwise mechanisms is within only a few kcal/mol. Thus, porphycene is an interesting molecular system that has competing dynamics of double proton transfer. Fig. 1 summarizes the porphycene tautomerization, showing the proton transfer pathways among the lowest four minimum structures. According to previous studies based on electronic structure calculations [11–22], the C_{2h} *trans* structure is the most stable tautomer and the C_{2v} *cis* structure is energetically higher than that of the *trans* structure. It is well-known that the D_{2h} structure is the transition state of the concerted pathway but it is the second-order saddle point on the potential energy surface. The transition state of the stepwise single proton transfer pathway between the D_{2h} and C_{2h} structures has the C_s symmetry with the first-order saddle point property.

* Corresponding author. Fax: +81 48 858 3700.
E-mail address: tako@mail.saitama-u.ac.jp (T. Takayanagi).

0301-0104/$ - see front matter © 2011 Elsevier B.V. All rights reserved.
doi:10.1016/j.chemphys.2011.12.007

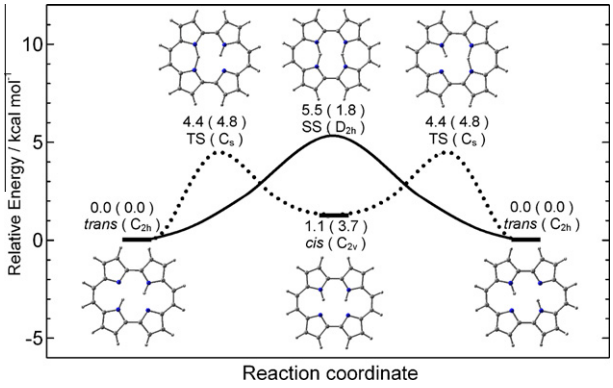

Fig. 1. Schematic potential energy diagram of the double proton transfer processes in porphycene obtained at the semiempirical PM6-SRP level. Concerted (C_{2h} *trans* ↔ D_{2h} second-order saddle point ↔ C_{2h} *trans*) and stepwise (C_{2h} *trans* ↔ C_s transition-state ↔ C_{2v} *cis*) double proton transfer pathways are shown. Numbers in parentheses indicate relative energies including zero-point vibrational energy corrections obtained from harmonic frequency analyses. The relative energy of the trans-porphycene (C_{2h}) is taken to be zero.

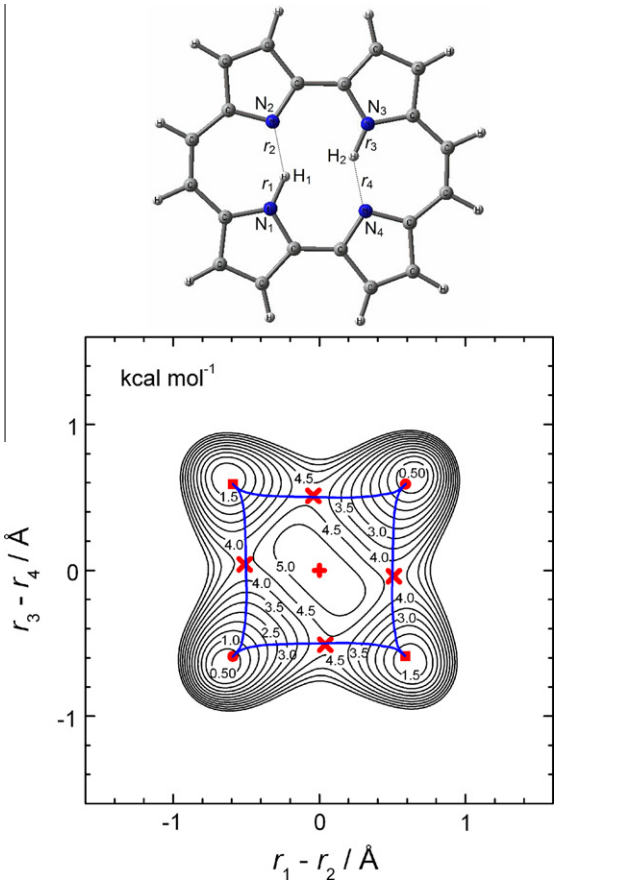

Fig. 2. Two-dimensional potential energy surface as a function of $r_1 - r_2$ and $r_3 - r_4$ coordinates obtained at the PM6-SRP semiempirical level, where r_i is the distance between the inner proton and nitrogen atom. Contour increments are set to 0.5 kcal/mol. Circles and squares indicate C_{2h} *trans* and C_{2v} *cis* minima, respectively. The saddle points for the stepwise process and the second-order saddle point for the concerted process are also shown as crosses. The intrinsic reaction coordinates for the stepwise process are also shown.

There have been many electronic structure calculations for the above-mentioned proton transfer pathways in porphycene [11–22]. Kozlowski et al. have carried out systematic calculations for the inner-proton migration of porphycene at the B3LYP and MP2 levels of theory [14]. They have theoretically shown that the C_{2v} *cis* intermediate structure is 2.4 kcal/mol higher in energy than the most stable C_{2h} *trans* structure at the B3LYP/TZ2P level without zero-point harmonic vibrational energy correction. Also, the barrier heights for the concerted and stepwise pathways were reported to be 7.6 and 4.9 kcal/mol at the B3LYP/TZ2P, respectively. This indicates that the stepwise mechanism is energetically favorable. However, it should be emphasized that zero-point vibrational energy correction significantly changes this energetic behavior. Kozlowski et al. have already pointed out that the barrier heights for the two pathways become comparable (~1.6 kcal/mol) after zero-point vibrational energy correction based on harmonic frequency analyses. This result comes from the fact that the D_{2h} second-order saddle point has one more imaginary frequency than the C_s first-order transition state structure. This implies that nuclear quantum effects could play an important role in the selection of dominant pathway of the proton transfer process as well as the reaction rate.

Motivated by the current status as mentioned above, we have recently reported preliminary computational results using full-dimensional path-integral molecular dynamics (PIMD) simulations, which can take both nuclear quantum and thermal fluctuation effects into account [23]. Since on-the-fly *ab initio* PIMD simulations were not computationally feasible for porphycene, we have alternatively employed the semiempirical electronic structure method whose semiempirical parameters were adjusted so as to reproduce the previously obtained energetics for the above-mentioned stationary points. It was found that the double proton transfer processes in porphycene dominantly occur via the concerted mechanism at $T = 300$ K. Based on the comparison between classical MD and PIMD calculations, it has also been concluded that the concerted pathway is emphasized by nuclear quantum effects. In this paper, we discuss the effect of isotopic substitution of the inner protons on the double proton transfer mechanism in porphycene.

2. Computational detail

Standard imaginary-time PIMD simulations [24,25] were performed to obtain thermal equilibrium structures including nuclear

Table 1
Relative energies of the stationary point configurations of porphycene with and without zero-point vibrational energy correction obtained on the PM6-SRP potential energy surface. Previous B3LYP and MP2 results are also presented for comparison. The energies are measured from the energy of the most stable C_{2h} *trans* structure.

Structure	Relative energy / kcal mol^{-1}						
	PM6-SRP[a]	B3LYP/6–31G(*d*,*p*)[a,b]	MP2/6–31 + G(*d*,*p*)[a,b]	HH[c]	DD[c]	HD[c]	HMu[c]
C_{2h} *trans*	0.0	0.0	0.0	0.0	0.0	0.0	0.0
C_{2v} *cis*	1.1	2.2	2.7	3.7	3.7	3.8	3.8
C_s transition-state	4.4	4.1	3.8	4.8	5.6	5.0	4.6
D_{2d} second-order saddle point	5.5	6.1	5.2	1.8	3.1	2.7	−2.5

[a] Relative energies without zero-point vibrational energy correction.
[b] Taken from Refs. [18,19].
[c] Relative energies with zero-point vibrational energy correction for isotopically substituted porphycenes on the PM6-SRP surface.

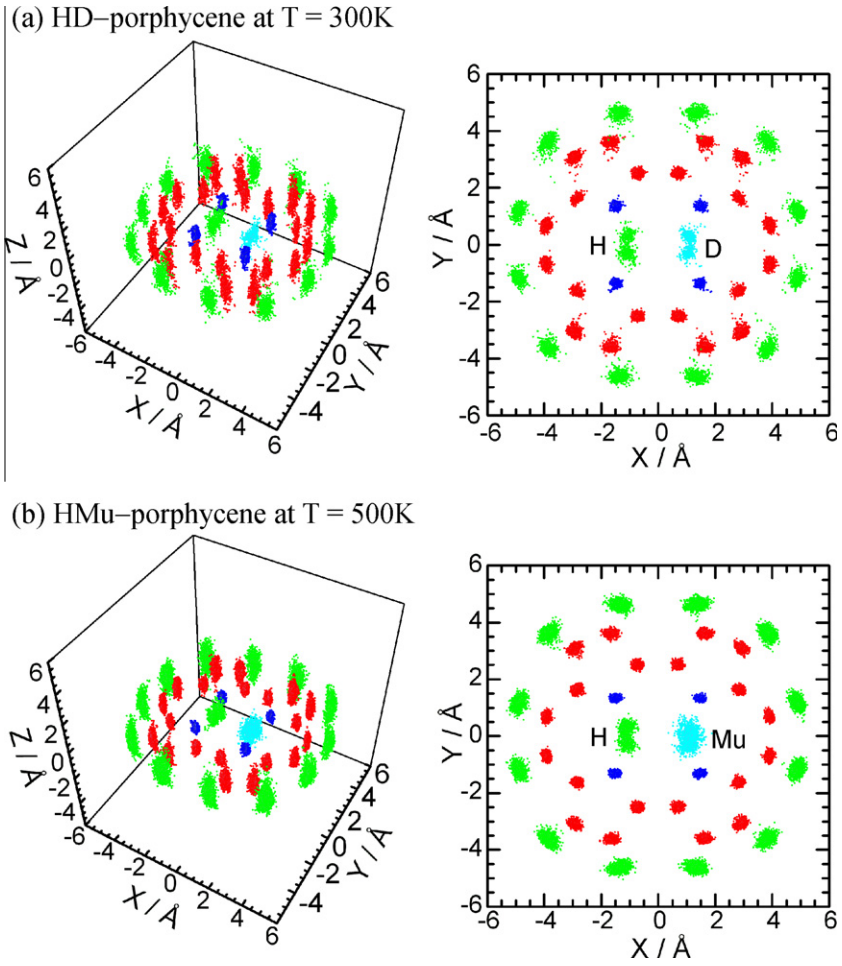

Fig. 3. Three-dimensional perspective plots of the PIMD nuclear distributions of the isotopically substitued porphycene molecules: (a) HD-porphycene at $T = 300$ K and (b) HMu-porphycene at $T = 500$ K. In both cases, one of the two inner protons of porphycene is isotopically substituted into deuteron or muon. Right panels show the distributions projected on the X–Y plane.

quantum effects directly using the potential energy values and their derivatives determined at the semiempirical PM6 level of theory [26] with adjusted semiempirical parameters. The semiempirical calculations were performed using the MOPAC2009 code [27], which has been interfaced to our PIMD simulation code. As mentioned in the previous section, the semiempirical parameters employed in the PM6 calculations were adjusted so as to qualitatively reproduce the previously reported energetics of the four stationary points (C_{2h} *trans* and C_{2v} *cis* minimum structures, D_{2h} second-order saddle point, and C_s first-order saddle point) on the ground-state potential energy surface of porphycene. Hereafter, we call this the PM6-SRP (specific-reaction-parameter [28–30]) potential energy surface. Detailed procedures for determining the parameters and the resulting values were already described in Ref. [23]. Here, the SRP parameters were determined referring to the structures and energies of previous electronic structure calculations at B3LYP/6–31G(d,p) and MP2/6–31 + G(d,p) levels of theory [18,19]. The stationary-point energy values obtained at the PM6-SRP level are presented in Fig. 1 and Table 1.

The PIMD simulations were carried out with $P = 24$–64 beads depending on the system temperature as well as isotopic substitution. The massive Nose–Hoover chain thermostat technique was implemented in the velocity Verlet algorithm to the control system temperature. The time increment was set to $\Delta t = 5$–10 atomic unit (0.12–0.24 fs). These numerical parameters were carefully chosen to obtain fully converged results. The details of our computational procedure are also described in Refs. [31–34].

3. Results and discussion

First, we mention the features of the PM6-SRP potential energy surface of porphycene we have employed. Fig. 2 displays the two-dimensional contour map plotted as a function of $r_1 - r_2$ and $r_3 - r_4$ distance differences, where r_i represents the N–H distance defined in the same figure. Notice that the $r_1 - r_2$ and $r_3 - r_4$ distances are able to characterize both concerted and stepwise pathways of the proton transfer reaction. All other internal coordinates were optimized with respect to total energy. Four potential minima are seen in Fig. 2 corresponding to the C_{2h} *trans* and C_{2v} *cis* structures; the two minima at $(-0.59, -0.59)$ and $(0.59, 0.59)$ correspond to the most stable C_{2h} *trans* structures, while the two minima at $(-0.59, 0.59)$ and $(0.59, -0.59)$ to the intermediate C_{2v} *cis* structures. Note that the relative energy is measured from the energy level of the C_{2h} *trans* minimum. The PM6-SRP potential gives the relative energy between the C_{2h} *trans* and C_{2v} *cis* structures to be 1.1 kcal/mol (see also Fig. 1 and Table 1). This value is somewhat smaller than the previously reported values obtained at the B3LYP/6–31(d,p) and *ab initio* MP2/6–31 + G(d,p) levels [14,18,19] but is close to the value obtained at the DFT–PBE level (1.5 kcal/mol) [20]. The barrier height for the first-order stepwise pathway (*trans–cis* interconversion) was obtained to be 4.4 kcal/mol at the PM6-SRP method, which is close to the B3LYP (4.1 kcal/mol) and MP2 (3.8 kcal/mol) values [18,19]. Notice that the corresponding transition states are seen at $(-0.51, 0.04)$, $(0.51, -0.04)$, $(-0.04, 0.51)$ and $(0.04, -0.51)$ in Fig. 2. The coordinate origin at

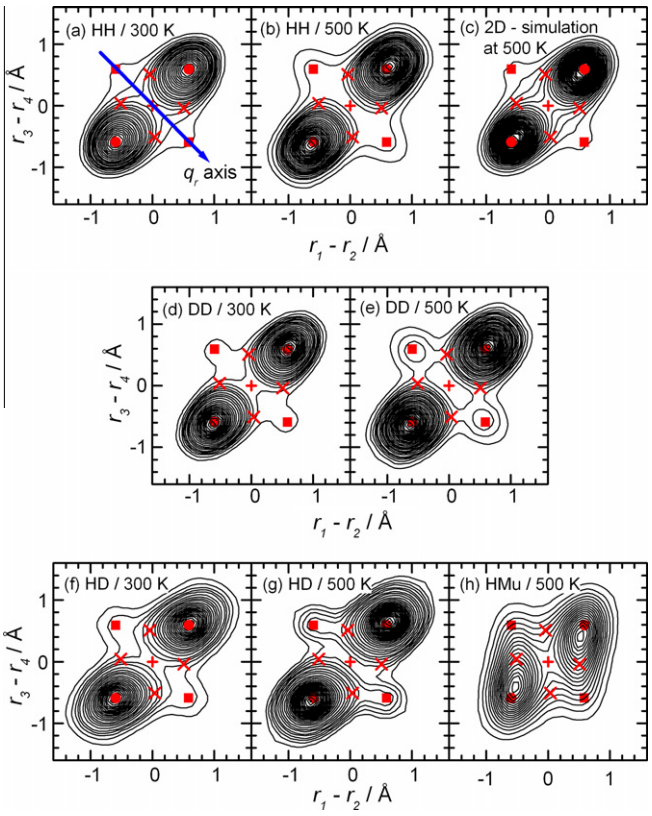

Fig. 4. Two-dimensional contour plots of the inner proton/deuteron distributions for prophycene and its isotopic variants as a function of $r_1 - r_2$ and $r_3 - r_4$ coordinates obtained from the PIMD simulations at $T = 300$ and 500 K. Symbols (circles, squares, and crosses) indicate the stationary points on the PM6-SRP potential energy surface. The result obtained from the 2D-PIMD simulation for HH-prophycene at $T = 500$ K with porphycene configurations being planar structures is also shown.

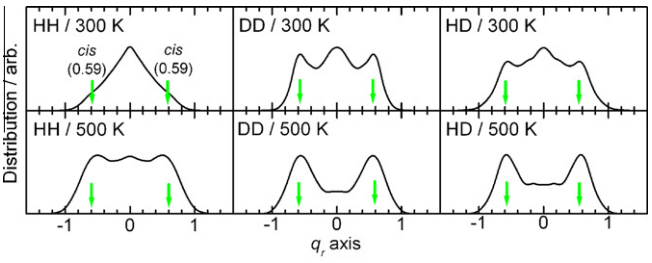

Fig. 5. Inner proton/deuteron distributions along the $r_1 - r_2 = r_4 - r_3$ line (corresponding to the q_r-axis in Fig. 4) obtained from the PIMD simulations at $T = 300$ and 500 K.

$r_1 - r_2 = r_3 - r_4 = 0$ corresponds to the D_{2h} second-order saddle point configuration of porphycene. The barrier height for the concerted pathway via the D_{2h} second-order saddle point is obtained to be 5.5 kcal/mol, which is thus slightly larger than the stepwise barrier height. Again, the obtained value is close to the previous B3LYP (6.1 kcal/mol) and MP2 (5.2 kcal/mol) results [14,18–20]. Of course, for a more reliable assessment, one should wait for *ab initio* calculations with higher accuracy to truly determine the barrier heights, such as CCSD(T) or MRCI level of theory with large basis sets. Such a calculation is not currently available, unfortunately, within our computer facility.

Next, we present the results of PIMD simulations. Fig. 3 shows representative three-dimensional perspective plots of the nuclear distributions obtained from the PIMD simulations for the isotopically substituted porphycene molecules, where one of the inner protons were replaced into deuteron (Fig. 3(a)) or muon (Fig. 3(b)), whose mass is about 1/9 of the proton mass. Notice that the Cartesian coordinates are transformed so as that overall translational and rotational motions are removed from this plot. Large fluctuation motion can be seen for both the inner proton and deuteron in Fig. 3(a), but the fluctuation for the inner proton is somewhat broader than that for the inner deuteron. Fig. 3(b) shows the nuclear distributions of the substituted porphycene, where one of the inner protons was replaced into muon. The corresponding PIMD simulation was performed with 64 beads at $T = 500$ K due to its very light mass of muon. It is interesting to note that the muon distribution is significantly broader than the proton distribution, and its density maximum is located around the midpoint of the two nitrogen atoms. This is simply because the zero-point energy of the corresponding muon vibration is very large. In this case, even when the potential energy surface has a double-minimum character, the particle is mainly located around the saddle point region. In fact, as is shown in Table 1, the zero-point corrected energy level of the D_{2h} structure is lower than that of the C_{2h} *trans* structure for the HMu-porphycene molecule within a harmonic approximation, which may be giving only qualitative and limited values.

In order to understand the effect of isotopic substitution as well as temperature on the double proton transfer mechanism in porphycene more clearly, we show two-dimensional contour plots of the inner proton/deuteron distributions as a function of the

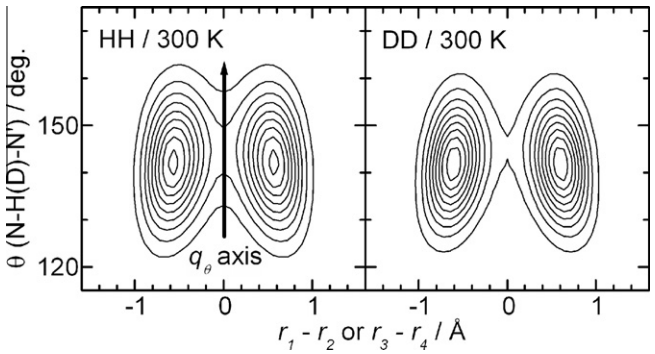

Fig. 6. Two-dimensional contour plots of proton/deuteron distributions for HH-porphycene and DD-porphycene as a function of $r_1 - r_2$ coordinate and angle θ (∠ N–H(D)–N) obtained from the PIMD simulations at $T = 300$ K.

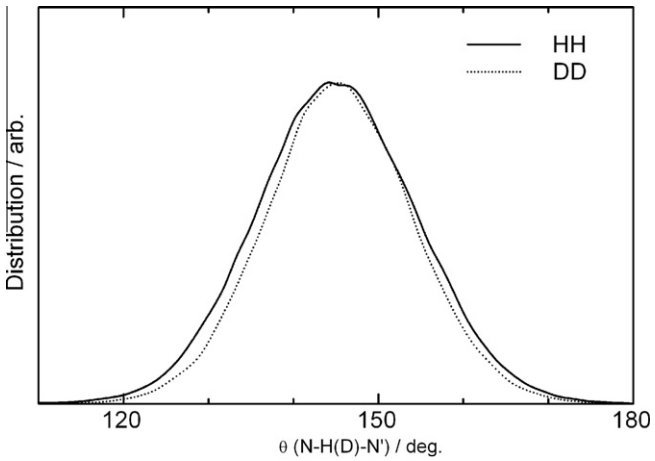

Fig. 7. Proton/deuteron distributions along the $r_1 - r_2 = 0$ line (corresponding to the q_0-axis in Fig. 6) for HH-porphycene and DD-porphycene obtained from the PIMD simulations at $T = 300$ K.

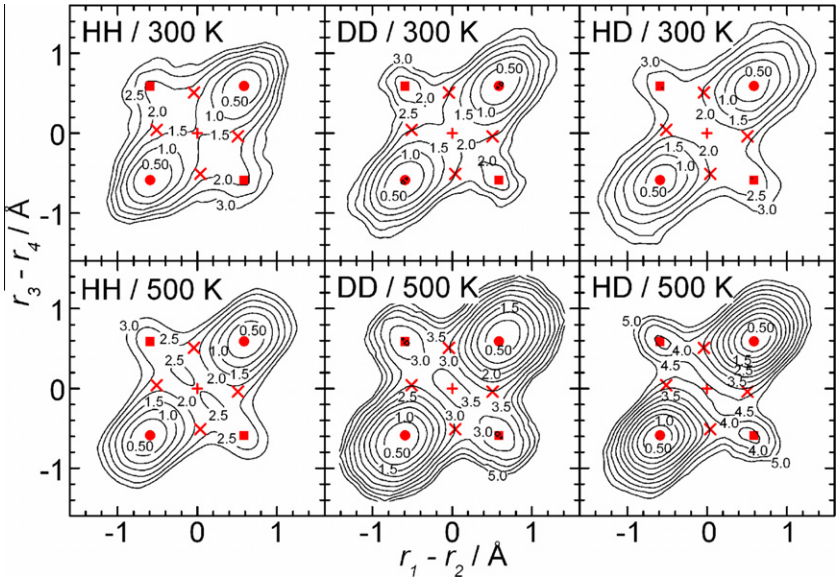

Fig. 8. Two-dimensional contour plots of free-energy surfaces as a function of $r_1 - r_2$ and $r_3 - r_4$ coordinates obtained from the PIMD simulations at $T = 300$ and 500 K for HH-porphycene, DD-porphycene, and HD-porphycene.

$r_1 - r_2$ and $r_3 - r_4$ coordinates in Fig. 4. In the case that one of the two inner protons is substituted by a deuteron (or muon), the $r_1 - r_2$ coordinate corresponds to the proton transfer motion while the $r_3 - r_4$ coordinate to the deuteron (muon) transfer motion. Fig. 5 shows the density distributions extracted along the straight line corresponding to $r_1 - r_2 = -(r_3 - r_4)$. Notice that this line intersects with both the C_{2v} *cis* minima and D_{2h} second-order saddle point. Thus, the density profile along this line gives the qualitative estimation of the contributions of the stepwise and concerted mechanisms. From the results presented in Figs. 4 and 5, we can clearly understand that double proton transfer between *trans–trans* structures for the unsubstituted porphycene (HH-porphycene) at $T = 300$ K mainly occurs through the concerted mechanism since the density distribution around the coordinate origin $(r_1 - r_2, r_3 - r_4) = (0,0)$ is relatively high. At the same time, it is seen that the population around the *cis* form is relatively low at $T = 300$ K, suggesting that the contribution of the stepwise mechanism is relatively small. On the other hand, in the case of the $T = 500$ K simulation, it is interesting to note that the population around the *cis* minimum significantly increases. This result indicates that the contribution of the stepwise double proton transfer mechanism increases as the temperature is increased for HH-porphycene.

Next we discuss the results obtained for isotopically substituted porphycenes. At $T = 300$ K, in the case that both the two protons are replaced by deuterons (DD-porphycene), the obtained distributions are similar to the unsubstituted HH-porphycene case although the density around the *cis* configuration is larger than that for the HH case. This suggests that the contribution of the stepwise mechanism becomes more important for the DD-porphycene molecule. Notice that the obtained distribution becomes asymmetric with respect to the $r_1 - r_2 = r_3 - r_4$ line when one proton is replaced by a deuteron (HD-porphycene) or muon (HMu-porphycene). It is interesting note that, in the HD-porphycene case at $T = 300$ K, the contribution of the concerted and stepwise mechanisms is seen to be comparable to the DD-porphycene case. Although the present PIMD simulations give only thermal statistical nuclear distributions, the asymmetric position of H and D must be relevant to the asynchronous motions of H and D transfer, and thus it should affect the trajectories of the reaction. Similar to the HH-porphycene case, it can be seen that the system temperature somewhat affects the density distributions, and hence the proton transfer mechanism.

Fig. 6 shows the two-dimensional contour plots of the inner proton/deuteron distributions as a function of the $r_1 - r_2$ coordinate and angle θ ($\angle$N–H(D)–N) obtained from the PIMD simulations at $T = 300$ K for the HH-porphycene and DD-porphycene molecules. It can be seen that the proton/deuteron transfer mainly occurs with bent configurations. Fig. 7 displays the distributions extracted along the $r_1 - r_2 = 0$ line from the distributions presented in Fig. 6. From these plots, one can see that the proton transfer occurs with a somewhat a wider range of θ than deuteron transfer.

In order to characterize the rate of chemical reactions, it is sometimes useful to compute a free energy surface $F(\boldsymbol{q})$ along an appropriate reaction coordinate $\boldsymbol{q}$ [34]. The free energy $F(\boldsymbol{q})$ is rigorously defined as $F(\boldsymbol{q}) = -k_B T \ln \rho(\boldsymbol{q})$, where $\rho(\boldsymbol{q})$ is the probability to observe a given value of $\boldsymbol{q}$ while sampling molecular configurations in the PIMD simulation. Fig. 8 shows the free energy surfaces associated with $r_1 - r_2$ and $r_3 - r_4$ coordinates. First, it should be emphasized that the features of all the free energy surfaces obtained are very different from those of the bare potential energy surface (see Fig. 2). In the case of HH-porphycene at $T = 300$ K, one can see that the free energy barrier (1.5 kcal/mol at the D_{2h} second-order saddle point) for the concerted pathway is lower than that for the *cis* configuration (1.8 kcal/mol at the *cis* minima). The former value is comparable to the zero-point energy corrected barrier height (1.8 kcal/mol) for the concerted pathway (see Table 1). At $T = 500$ K, the free energy barrier for the concerted pathway is estimated to be ~2.5 kcal/mol for HH-porphycene. Thus, the free energy barrier is higher for the concerted pathway as the temperature is higher. One of the important origins for this temperature dependence in the barrier height may be large quantum fluctuation at lower temperatures, which is characterized by the radius of gyration of the ring polymer in the transition state [35]. However, further analysis must be done to study this issue in detail, which is beyond our scope here.

As an independent issue from the discussions above, another interesting one is on the role of broken planarity of the porphycene molecule at finite temperatures. In order to investigate this issue, we have also performed similar PIMD simulations with the porphycene configurations restricted to be always planer (hereafter, we call it "2D-PIMD"). Fig. 4(c) displays the nuclear distribution plotted as a function of the $r_1 - r_2$ and $r_3 - r_4$ coordinates obtained

from the 2D-PIMD simulations at $T = 500$ K. Compared with the "3D-simulations" at $T = 500$ K presented in Fig. 4(b), the concerted proton transfer mechanism is enhanced while the stepwise mechanism is somewhat suppressed in the 2D-simulation. This result qualitatively suggests that the out-of-plane motions of porphycene have the influence of suppressing the concerted proton transfer mechanism. In this case, the out-of-plane motions could be considered as mainly entropic effects since the vibrational frequencies of the corresponding normal modes are in the range of 50–200 cm^{-1} which is smaller than thermal energy, k_BT. Recently, there has been an interesting experimental report by Vdovin et al. [8] that for porphycene embedded in superfluid helium nanodroplets there are vibrational modes that enhance and suppress the concerted proton transfer tunneling probability. In order to fully address this experimental finding from the theoretical side, a quantum dynamics study including various vibrational modes should be carried out. This is an important future direction.

4. Conclusions

In this work we have carried out quantum PIMD simulations in order to theoretically understand the inner double proton/deuteron transfer mechanisms of porphycene and its isotopic variants. We have used the on-the-fly direct dynamics technique at the semiempirical PM6 molecular orbital level but with its semiempirical parameters being adjusted so as that the stationary point energetics reproduces previous *ab initio* and DFT results reasonably. Using this technique, we were able to sample molecular configurations large enough for discussing the proton transfer mechanism from a quantum mechanical perspective. Although our PIMD simulation does not provide information about the dynamics in real-time, it has been successful to derive some important conclusions on the double proton transfer mechanism in porphycene.

The PIMD simulation for the unsubstituted HH-porphycene at $T = 300$ K shows that the double proton transfer mechanism dominantly occurs through the concerted pathway via configurations around the D_{2h} second-order saddle point. This result is in high contrast with the previous classical simulation results. At $T = 500$ K, the contribution of the stepwise mechanism significantly increases. It was found that the isotopic substitution of the inner protons into deuterons affects the transfer mechanism. We have also carried out the PIMD simulation for HH-porphycene at $T = 500$ K with the porphycene molecular configurations restricting planar structures. Interestingly, this simulation shows that the contribution of the stepwise mechanism decreases compared to the full-dimensional simulation result at the same temperature. From this result, we can qualitatively conclude that out-of-plane vibrational motions suppress the concerted mechanism presumably due to entropic effects.

Finally, we would like to give some comments on the accuracy of the PM6-SRP potential energy surface. The present PM6-SRP potential energy surface has been modeled so as to give reasonable agreement with the previous electronic structure results; however, it should be emphasized that the PM6-SRP surface still has large uncertainty in accuracy since highly accurate benchmark electronic structure calculations have not yet been available for porphycene. Thus, the present quantum simulation results are still preliminary and more accurate *ab initio* path-integral simulations should be made to fully confirm the validity of the conclusions obtained here. Nevertheless, we hope that the present simulations stimulate future experimental and theoretical studies for understanding the double proton transfer mechanisms of porphycene and its isotopic variants.

Acknowledgments

We would like to thank Grant-in-Aid for Scientific Research and for the priority area by Ministry of Education, Culture, Sports, Science and Technology, Japan.

References

[1] K. Giese, M. Petković, H. Naundorf, O. Kühn, Phys. Rep. 430 (2006) 211.
[2] J.T. Hynes, J.P. Klinman, H.H. Limbach, R.L. Schowen, Hydrogen-Transfer Reactions, Wiley-VCH, Weinheim, Germany, 2007.
[3] J. Waluk, Acc. Chem. Res. 39 (2006) 945.
[4] E. Vogel, M. Köcher, H. Schmickler, J. Lex, Angew. Chem. Int. Ed. Engl. 25 (1986) 257.
[5] J. Waluk, M. Müller, P. Swiderek, M. Köcher, E. Vogel, G. Hohlneicher, J. Michl, J. Am. Chem. Soc. 113 (1991) 5511.
[6] J. Sepioł, Y. Stepanenko, A. Vdovin, A. Mordziński, E. Vogel, J. Waluk, Chem. Phys. Lett. 296 (1998) 549.
[7] A. Vdovin, J. Sepioł, N. Urbańska, M. Pietraszkiewicz, A. Mordziński, J. Waluk, J. Am. Chem. Soc. 128 (2006) 2577.
[8] A. Vdovin, J. Waluk, B. Dick, A. Slenczka, Chem. Phys. Chem. 10 (2009) 761.
[9] M. Gil, J. Waluk, J. Am. Chem. Soc. 129 (2007) 1335.
[10] B. Wehrle, H.-H. Limbach, M. Köcher, O. Ermer, E. Vogel, Angew. Chem. Int. Ed. Engl. 26 (1987) 934.
[11] Y.D. Wu, K.W.K. Chan, C.P. Yip, E. Vogel, D.A. Plattner, K.N. Houk, J. Org. Chem. 62 (1997) 9240.
[12] K. Malsch, G. Hohlneicher, J. Phys. Chem. A 102 (1997) 8409.
[13] M. Boronat, E. Ortí, P.M. Viruela, F. Tomás, J. Mol. Struct. (THEOCHEM) 390 (1997) 149.
[14] P.M. Kozlowski, M.Z. Zgierski, J. Baker, J. Chem. Phys. 109 (1998) 5905.
[15] M.F. Shibl, M. Tachikawa, O. Kühn, Phys. Chem. Chem. Phys. 7 (2005) 1368.
[16] H. Cybulski, M. Pecul, T. Helgaker, M. Jaszuński, J. Phys. Chem. A 109 (2005) 4162.
[17] T. Udagawa, M. Tachikawa, J. Chem. Phys. 125 (2006) 244105.
[18] Ł. Walewski, D. Krachtus, S. Fischer, J.C. Smith, P. Bała, B. Lesyng, Int. J. Quant. Chem. 106 (2006) 636.
[19] Z. Smedarchina, M.F. Shibl, O. Kühn, A. Fernández-Ramos, Chem. Phys. Lett. 436 (2007) 314.
[20] Ł. Walewski, P. Bała, B. Lesyng, NIC Ser. 36 (2007) 291.
[21] M.F. Shibl, M. Pietrzak, H.H. Limbach, O. Kühn, Chem. Phys. Chem. 8 (2007) 315.
[22] Ł. Walewski, J. Waluk, B. Lesyng, J. Phys. Chem. A 114 (2010) 2313.
[23] T. Yoshikawa, S. Sugawara, T. Takayanagi, M. Shiga, M. Tachikawa, Chem. Phys. Lett. 496 (2010) 14.
[24] D. Marx, M. Parrinello, Z. Phys. B 95 (1994) 143.
[25] B.J. Berne, D. Thirumalai, Ann. Rev. Phys. Chem. 37 (1986) 401.
[26] J.J.P. Stewart, J. Mol. Model. 13 (2007) 1173.
[27] J.J.P. Stewart, *MOPAC2007*, Stewart Computational Chemistry, Colorado Springs, CO, USA, http://www.OpenMOPAC.net (2007).
[28] A. Gonzalez-Lafont, T.N. Truong, D.G. Truhlar, J. Phys. Chem. 95 (1991) 4618.
[29] Y.P. Liu, D.H. Lu, A. Gonzalez-Lafont, D.G. Truhlar, B.C. Garrett, J. Am. Chem. Soc. 115 (1993) 7806.
[30] T. Rossi, D.G. Truhlar, Chem. Phys. Lett. 233 (1995) 231.
[31] M. Shiga, M. Tachikawa, S. Miura, Chem. Phys. Lett. 332 (2000) 396.
[32] M. Shiga, M. Tachikawa, S. Miura, J. Chem. Phys. 115 (2001) 9149.
[33] M. Shiga, M. Tachikawa, Chem. Phys. Lett. 374 (2003) 229.
[34] U.W. Schmitt, G.A. Voth, J. Chem. Phys. 111 (1999) 9361.
[35] M.J. Gillan, Phys. Rev. Lett. 58 (1987) 563.